Chapter 5

Continuous record of microparticle concentration and size distribution in the central Greenland NGRIP ice core during the last glacial period

Urs Ruth, Dietmar Wagenbach, and Jørgen P. Steffensen

Submitted to *Journal of Geophysical Research*

Continuous record of microparticle concentration and size distribution in the central Greenland NGRIP ice core during the last glacial period

Urs Ruth[1,2], Dietmar Wagenbach[1], and Jørgen P. Steffensen[3]

[1]Institut für Umweltphysik, University of Heidelberg, Germany
[2]Alfred Wegener Institut für Polar- und Meeresforschung, Bremerhaven, Germany
[3]Department of Geophysics, University of Copenhagen, Denmark

Abstract The application of a novel laser particle detector in conjunction with controlled longitudinal sample melting has provided a more than 1500 m long continuous record of microparticle concentration and size distribution of the NGRIP ice core. The resulting profile has a depth resolution of 1.65 m and covers almost the complete last glacial period. The microparticle concentration increases by a factor of 100 in the Last Glacial Maximum (LGM) compared to the Preboreal. At rapid climatic transitions sharp variations of the concentration occur synchronously with changes of the $\delta^{18}O$ temperature proxy. The lognormal mode μ of the volume distribution also shows clear systematic variations with smaller particles during warmer climates. We find $\mu \approx 1.7$ μm diameter during LGM and $\mu \approx 1.3$ μm during the Preboreal. During warm periods μ was more variable as reflected by increased point-to-point variability and also by increased values of the standard deviation of the distribution for the multi-year samples considered here. On timescales below several 100 years μ and the particle concentration exhibit a certain degree of independence noticeable especially during warm periods. Using highly simplifying considerations of the atmospheric dust cycle we find that (i) the observed changes of μ in the ice largely reflect changed airborne particle sizes above the ice sheet and (ii) that changes of μ are indicative for changes of atmospheric long range transport times. From the observed size changes we deduce roughly 25% shorter transit times during LGM compared to the Preboreal. The associated concentration increase from this change is roughly estimated to less than one order of magnitude.

Introduction

Ice cores provide a wealth of paleoclimatic information including records of windblown mineral aerosol (hereinafter also called dust). Among all deposited components this atmospheric constituent has a special quality because not only its concentration but also the size distribution of its insoluble fraction is preserved. As East Asian deserts have been identified as the most probable source area for dust transported to Greenland [*Biscaye et al.*, 1997; *Kahl et al.*, 1997; *Svensson et al.*, 2000] long range atmospheric transport plays a central role in the dust cycle. Therefore, archives of the dust aerosol may hold specific information about atmospheric transport in particular.

Mineral dust concentrations in ice cores exhibit a large dynamic variation throughout a climatic cycle. Dust concentrations vary by a factor of $\approx$100 between the Holocene and the Last Glacial Maximum (LGM) in central Greenlandic ice [*Steffensen*, 1997]. From continuous microparticle and Ca^{2+} measurements in the Renland ice core [*Hansson*, 1994] and on the basis of continuous Ca^{2+} records from the GRIP ice core [*Fuhrer et al.*, 1999] it was demonstrated that at rapid climatic transitions the dust concentration varied synchronously with the $\delta^{18}O$ temperature proxy. While early explanations for the pronounced increase in dust concentration suggested the importance of exposed continental shelves due to a lower sea level during the last glacial [*Cragin et al.*, 1977; *Hammer et al.*, 1985], more recent work negates this idea [*Steffensen*, 1997] and rather points to changed atmospheric conditions [*Petit et al.*, 1981; *Petit et al.*, 1990] and intensified sources [*Fuhrer et al.*, 1999]. Further specification of this general inference remains difficult as the observed dust concentrations are a combined result of a number of entangled mechanisms ranging from dust mobilization in the source areas over uplift and long range transport to deposition onto the ice sheet.

Fuhrer et al. [1999] have addressed some of the involved processes, but the fact that changes of source aridity, surface wind speed, uplift, transport, and deposition may all have been variable on similar timescales and also synchronized [*Porter and Zhisheng*, 1995; *Wang et al.*, 2001] makes it very difficult to separate individual processes. As yet, only rough estimates can be expected from modelling approaches because dust models - although having improved considerably - are still barely reproducing the concentration change observed in polar archives and cannot confidently resolve the individual processes involved [*Andersen et al.*, 1998; *Mahowald et al.*, 1999; *Tegen and Rind*, 2000]. Also, models are so far unable to describe mixing mechanisms in the lower boundary layer at the ice sheet which are important for the deposition process.

Size distribution measurements on the insoluble fraction of dust in polar ice cores have shown that the majority of the particle mass can be described by a lognormal

distribution with a modal diameter around 1.5 to 2.0 μm [*Royer et al.*, 1983]. This mode is found to be fairly robust in remote regions world wide. But small systematic shifts have been observed on various time scales in ice cores from Greenland as well as from Antarctica, e.g. [*Steffensen*, 1997; *Delmonte et al.*, 2002]. As particle size distributions may be indicative for atmospheric circulation it may be possible to use this information to gain further insights into the past dust cycle. But size distribution measurements are scarce. So far they have been performed only in a discontinuous spot check manner using microscopy or the well established Coulter counting technique. For Greenland, *Steffensen* [1997] finds a tendency towards larger lognormal modes for colder climates, which are associated with higher dust concentrations.

The interpretation of the observed particle sizes is not straight forward. It is known that depletion processes during long range transport are generally size fractionating [*Junge*, 1977], that size altering in-cloud processing may occur [*Wurzler et al.*, 2000], and that the deposition process to the ice sheet bares the potential of changing the size distribution [*Unnerstad and Hansson*, 2001]. But a quantification of these processes is difficult, and our current understanding about how different climatic situations may have influenced the particle size distribution is limited. Also, the forward modelling of particle size distributions is not very accurate. Dust modules for general circulation models (GCM) work with one or only few size classes (e.g. four classes covering the range from 1 to 100 μm [*Tegen and Fung*, 1994]) and cannot resolve fine shifts of the lognormal mode.

So far, no continuous profile covering the last glacial period has been provided from ice cores for microparticle size distribution parameters. In particular, it is unclear how the size distribution behaved at fast climatic transitions. Also, possible inferences from changed size distributions for atmospheric circulation changes are not well understood.

Here we present a comprehensive data set from the North Greenland Ice Core Project (NGRIP) deep ice core, drilled at (75.1N, 42.3W) in central Greenland about 300 km north of the summit region. The record is approximately from 1400 m to 2930 m depth and covers continuously the period from $\approx$9.5 kyr before present (bp) to $\approx$100 kyr bp, i.e. it includes the Pleistocene to Holocene transition and almost the complete ultimate glacial period. The core was analyzed continuously for insoluble microparticle concentration and size distribution deploying a novel laser based sensor. This sensor is not as delicate and does not require as extensive sample preparation as a Coulter Counter, which makes it possible to acquire a continuous profile over this long depth interval. To find an interpretation of the observed size changes, we present a simple model picture that that describes the modification of a particle size distribution during long range transport and deposition.

Methods

Measurements The measurement procedure and the laser based particle detector have already been described by [*Ruth et al.*, 2002] and therefore are only briefly outlined here. However, the aspect of the size calibration will be covered in greater detail. The measurements took place in a warm laboratory during the NGRIP-2000 field campaign. Continuous sections of core were melted in a controlled fashion along the core direction. The melt water was subjected to established continuous flow analysis (CFA) systems (e.g. [*Röthlisberger et al.*, 2000]; M. Bigler, *Dissertation in preparation*, University of Berne) and to particle analysis, which all work on a flow-through basis. For decontamination purposes the abutting faces of the core sections were carefully cleaned using a stainless steel microtome blade. In addition, the melter had two concentric sections, and only the uncontaminated meltwater from the inner section was used for the analyses as described by *Röthlisberger et al.* [2000]. Peristaltic pumps and teflon tubings were used to feed the water into the detection units. Debubblers were used to eliminate air bubbles.

In our measuring procedure the size distribution data was accumulated over 1.65 m intervals, while the particle concentration may also be recorded at an effective depth resolution of 1.0 cm [*Ruth et al.*, 2002]. Count rates were transformed to concentrations by means of regular flow rate measurements. To avoid coincidence distortion of the particle counting the sample water of glacial ice was diluted with prefiltered (0.2 μm) carrier water. Dilution was performed below 1494.9 m depth, i.e. for ice from the Younger Dryas period and older. The total sample volume consumed for a 1.65 m long section was approximately 6 ml.

Size calibration of the particle sensor The particle detection is based on laser light attenuation by single particles. The sample water is pumped through an illuminated detection cell, where each particle is detected as a negative peak of transmitted light. The peaks are counted and sorted by height into channels, that can be adjusted to appropriate size intervals. 12 channels were used in this application.

The interrelation of peak height and particle size is complex as both geometric shadowing and scattering processes are involved. Shadowing depends on geometric particle cross section, and therefore on a combination of particle volume, shape and orientation. Scattering in addition depends on optical particle properties and features nonlinearities between particle size and scattered light intensity. Only in the upper end of the size spectrum geometric shadowing dominates enough to allow a calibration with latex spheres of known diameter. In the remaining main part of the spectrum

scattering becomes increasingly important, and a size calibration with latex spheres is inaccurate because mineral aerosol particles have different scattering properties than latex spheres of identical volume, predominantly due to their non-spherical shape [*Saey*, 1998].

Therefore, a size calibration was achieved indirectly through a comparison with measurements using a Coulter Counter, which measures the particle volume directly and independently of shape. At selected horizons, NGRIP ice core samples were also measured with a Coulter Counter, and subsequently the laser sensor size axis was adjusted until the laser sensor data and the Coulter Counter data showed optimal correspondence. Samples from five different climatic periods (Preboreal Holocene, Younger Dryas (YD), Allerød, LGM, and pre-LGM cold glacial (CG)) were used for the calibration, thus the full concentration range was covered.

During the calibration process it was discovered that the dilution setup had had a modifying influence on the size distribution. Therefore, the measurements of Preboreal Holocene ice (without dilution setup) and glacial ice (with dilution setup) were calibrated separately. Figure 1 shows the volume distribution spectra used for the two calibrations. The Preboreal sample was used to calibrate the measurements above 1494.9 m depth, that were done without sample dilution (A). For the calibration of the measurements below this depth the other four samples were used (B). After the adjustment of the laser sensor size axis, the data sets of the two counters show good accordance. Differences between the laser sensor and the Coulter Counter data may result from the fact that the Coulter Counter data covers only 0.55 m out of the 1.65 m long section measured with the laser sensor so that the underlying size distributions possibly indeed slightly differed in the respective samples. For calibration (B) the differences in the underlying sample populations counterbalance each other as several horizons could be used for one calibration.

Data parametrization A lognormal function was used to parametrize the volume distribution data:

$$\frac{dV}{d\ln d} = \frac{V_0}{\sqrt{2\pi}\ln\sigma} e^{-\frac{1}{2}\left(\frac{\ln d - \ln \mu}{\ln \sigma}\right)^2},$$

where V_0 is the amplitude, μ the mode and σ the standard deviation of the distribution (herein also called 'lognormal mode' and 'lognormal standard deviation' for simplicity). Because the width of the size channels was quite large the fit procedure regarded the distribution within each channel. Furthermore, the fitting procedure was such that not the absolute but the relative quadratic error was minimized in order to put equal weight on all channels. The first nine channels were considered for fitting, i.e. particles

between 1.0 μm and 7.5 μm diameter.

Other parameters are sometimes taken to characterize a particle size distribution: The volume V_c of coarse particles ($d > d_c$) is used as well as the relative coarseness as V_c/V_{tot}; d_c was chosen to 7.5 μm in our study. The parameters 'mean volume diameter' (MVD) and 'mean number diameter' (MND) as e.g. used by [*Zielinski*, 1997] denote the mean diameter with respect to volume or number. As they highly depend on the measuring range and thus are intercomparable only for identically treated data sets we do not discuss them here. Furthermore, the MVD was found to be ambiguous in our data: At high dust concentrations it tended to be in phase with changes of the lognormal mode μ and in antiphase with the relative coarseness (i.e. it depended on the size of small particles); yet at low concentrations it tended to be in antiphase with the mode and in phase with relative coarseness (i.e. it depended on the abundance of large particles).

Because a considerable portion of the microparticle mass is contributed by the small particles below the detection limit of approximately 1.0 μm, insoluble microparticle mass concentrations reported in this paper are derived as follows: For $d > \mu$ the total measured particle volume $V_m^{d>\mu}$ is taken by summation of all relevant channels or fractions thereof; below the mode the volume is taken from the fitted lognormal distribution, i.e. $V_{tot} = V_m^{d>\mu} + 0.5 \cdot V_0$. Subsequently, the total mass concentration is inferred by assuming a material density of 2.6 g cm^{-3} [*Sugimae*, 1984].

Measurement errors Occasionally, sections were affected from system malfunction. These could be identified from laboratory log entries and unrealistically strong excursions of the MND and were excluded from further processing. Few sections showed a very high concentration of large particles possibly resulting from contamination and were also excluded. The measurement blank for small particles was below 15% of the count rate for most low concentration samples and was negligible in high concentration samples; for coarse particles the measurement blank relative to the particle count rate was higher and more variable. Since for coarse particles also counting statistics deteriorate caution must be taken when interpreting the volume of the coarse fraction. The error of the total number concentration for all particles is predominantly due to flow rate uncertainties and is estimated to typically 5% - 10%. The uncertainty of total volume or mass concentration as due to flow rate and size calibration uncertainties is estimated to be about 15% - 20%.

The determination of the particle size is hindered through the influence of the flow set up on the size distribution, which may not be constant and therefore not at all times be fully compensated for by the calibration. Further, the calibration is affected

from the fact that the Coulter Counter data covers only part of the sample population measured with the laser sensor, which may explain the difference of about 0.1 μm between the fit parameter μ when derived from the Coulter Counter or the laser sensor data (see Figure 1). The difference in μ that result from using calibration A or B for any given sample was typically around 0.04 μm. The analytical uncertainty of the fit is variable and lies in the range from 0.01 μm to 0.1 μm diameter. We therefore estimate the possible error for μ to be generally around 0.1 μm diameter; it may be larger for the Holocene samples, where only one calibration horizon exists and also the uncertainty of the fit is large. Double measurements on ice from the YD-Holocene transition, one time performed without and the other time with the dilution setup, yielded a discrepancy in μ of up to 0.1 μm, which supports the above estimates.

The laser sensor was easy to handle and proved suitable for deployment under field conditions. It was possible to calibrate the laser sensor for proper sizing of windblown mineral dust particles. In future usage the flow system between melter and sensor should be as short as possible and kept unchanged throughout the measurements. Calibrations should be based on multiple horizons from different climatic periods, where applicable.

Results

Size distributions Four individual volume size distributions are shown in Figure 2 for illustration. They are representative for different climatic periods, namely LGM (a), Stadial (S) S9 (b), Interstadial (IS) IS10 (c), and Preboreal Holocene (d). The samples span a concentration range of more than two orders of magnitude for particles smaller than 7.5 μm. For coarse particles larger than 7.5 μm the concentration range of the four samples is less than one order of magnitude and is not strictly correlated to the concentration of small particles.

The respective lognormal fits are also shown in Figure 2, and the position and uncertainty of the lognormal mode μ are indicated. The fits describe the measured distributions very well for high concentration samples. For low concentration samples the description is still satisfactory, however deviations of the data from the ideal model distribution are larger. It may also be noticed that for higher concentration samples the position of the mode tends to increase whereas the width of the distribution tends to decrease.

Profiles Particle concentration and size distribution parameters of all samples are plotted as depth profiles in Figure 3. Shown are the insoluble particle number concen-

tration C_N, mass concentration C_M, lognormal mode μ of the volume distribution, and lognormal standard deviation σ. The concentration profiles clearly exhibit all climatic events known from the Greenlandic GRIP and GISP2 deep ice core records [*Johnsen et al.*, 1997; *Grootes and Stuiver*, 1997], some of which have been labeled in the figure. In particular, the stadial-interstadial fluctuations (or Dansgaard-Oeschger (D/O)-events) are clearly resolved. Periods of low particle concentrations correspond to warm phases while cold phases correspond to high particle concentrations. Concentrations are lowest during Preboreal Holocene ($C_N \approx 1 \cdot 10^4$ ml^{-1} or $C_M \approx 70$ μg kg^{-1}) and highest during LGM ($C_N \approx 1 \cdot 10^6$ ml^{-1} or $C_M \approx 8000$ μg kg^{-1}). This compares well to the reported microparticle mass concentrations from the GRIP core of 50 μg kg^{-1} and 8000 μg kg^{-1} for Preboreal and peak-LGM respectively [*Steffensen*, 1997]. Discrepancies to the GRIP data may be due to differences in the methods of measurement and data evaluation and need not be of geographical origin. The relative changes of the mass concentrations across D/O-transitions range from a factor of 5 to 18 and are typically around 8.

The overall appearance of the insoluble microparticle concentration profile as expected resembles much the continuous Ca^{2+} concentration profile from the GRIP core [*Fuhrer et al.*, 1999]. This means that the soluble and insoluble parts of the mineral aerosol varied largely alike. However, systematic changes of the Ca^{2+}/microparticle ratio by a factor ≤ 2 may be expected [*Steffensen*, 1997; *Ruth et al.*, 2002].

The close correspondence of the microparticle profile to the GRIP Ca^{2+} or $\delta^{18}O$ profiles permits to establish a provisional timescale for our NGRIP microparticle data by matching respective climatic events and subsequently transferring the GRIP SS09 timescale [*Johnsen et al.*, 1997] to the NGRIP core. Thereby we infer that the time coverage of each 1.65 m section ranges between 35 and 200 years. We also find that the concentration changes at D/O-transitions may have happened within 100 years or less.

Also the mode μ shows considerable systematic variability throughout the record, and most major climatic events as identified from the concentration profiles are also visible in the size distribution. These are in particular the YD and B/A periods, and the more prominent D/O-events; but also smaller D/O-events or the LGM as a whole are identifiable in the profile. Typical values for μ in the Preboreal are around 1.3 μmdiameter; and peak values exceed 1.7 μm during LGM. Typical values within the Pleistocene are around 1.6 μm during cold periods and may decrease to values around 1.4 μm or less during interstadial warm periods. A marked increase of the mode can be noticed between 2600 m and 2500 m depth, which corresponds to the transition from Marine Isotope Stage (MIS) 5 to MIS 4. Below this depth (i.e. during MIS 5) μ

was generally about 0.2 μm smaller than above. During corresponding periods we find roughly 0.2 μm smaller modes than *Steffensen* [1997] does for selected periods in the GRIP ice core.

The switching of the mode between states may happen as fast as the concentration changes, but it is not always as evident. Further, μ tends to be more variable (point-to-point variation) when crustal concentrations are low. This higher variability persists even when the data is averaged to equally long time periods; so it is not a consequence from formal counting statistics nor from the fact that low concentration samples systematically cover shorter time spans.

The lognormal standard deviation also shows systematic variations. It ranges from about 1.55 during LGM to more than 2 during the warm periods of MIS 5. It tends to be high when μ shows a large point-to-point variability. This indicates that at these times the mode was more variable also *within* each 1.65 m section.

Systematic changes of the mode In Figure 3 it is observed that the mode tends to increase for large particle concentrations. A systematic plot of these two parameters is shown in Figure 4a, where the data shown is averaged to 200 years resolution to reduce the point-to-point scatter for periods with higher layer thickness. A clear positive correlation is exhibited. It also can be noted that the spread of the mode is by about a factor of 3 smaller for high than for low particle concentrations. Larger modes and smaller spread for high concentration samples are also observed if the data is averaged over climatic periods (Figure 4b).

Detailed profile section A closer look at rapid transitions may bring further insights into the dust regime. Figure 5 shows the zoomed profile from IS 9 through IS 12 with size distribution parameters, particle concentration, and δ^{18}O (isotope data: personal communication from NGRIP-members, unpublished data). Cold periods very clearly show high dust concentrations and vice versa. Further, almost all high concentration periods are concurrent with large modes; however, not all periods with low concentrations are accompanied by smaller modes, and during low concentration periods the mode is more variable. This shows an independence of μ and V which is especially pronounced during warm periods.

The fact that the mode is more variable during warm periods may cause confusion when determining the exact point of a transition. One such occasion at the beginning of IS 11 is marked in Figure 5 with an arrow. Here, the size distribution shifts synchronously with the concentration into the "warm"-state as can be seen from the profile of σ. However, its increased variability allows the mode to stay large for two more sam-

ples (corresponding to roughly 200 years). Only the increased values for σ show that the individual dust events contributing to the multi-year samples were already more variable with respect to particle size, as is typical for warm periods. Therefore, σ is a more reliable parameter than μ when the exact point of a D/O-transition needs to be determined from size distribution parameters on the basis of multi-year samples.

Another observation is that there may indeed be a difference in the particular time when a transition occurs in the concentration and in the size distribution of microparticles (circles in Figure 5). No systematic leads or lags seem to occur, but shifts range up to $\pm$200 years. This again shows some independence of the processes influencing the particle concentration or size distribution. Such processes may have included variations of source strength and the amount of non-sizefractionating depletion processes during transport (see below). The independence is observed especially during warm periods, and it vanishes if the data is averaged for several centuries.

A simple model picture

The atmospheric dust cycle starts with the production of small sized wind-deflatable material in the source areas by weathering processes [*Pye*, 1987]. The amount of entrained dust depends on the occurrence and strength of surface winds, the size of the source areas and the mobility of the dust therein [*Gillette et al.*, 1980]. The geographical overlap of source region and long range transport zones may be another important factor [*Chylek et al.*, 2001]. The transport of dust depends on long range transport patterns, which in turn are influenced by e.g. global heat distribution or the ice cover of land and ocean [*Krinner and Genthon*, 1998]. Transport efficiency depends on sink processes leading to particle loss en route. Finally, the deposition of microparticles onto the ice sheet depends on wet and dry deposition processes [*Davidson et al.*, 1996].

In the following we will elucidate the potential of some of these processes to change the size distribution of an ensemble of particles. We will investigate to what extent the observed size distribution changes of microparticles may be due to changed deposition conditions during different climates, and how atmospheric circulation needs to have been different to account for the remaining size change. Hereby, our very simple approach clearly is far from capturing reality in all its complexity; but at least the direction of effects should be confidently resolved, and rough estimates of the magnitude of effects may be gained.

For comparison of two climatic states in the following sections we use the upper index '*cold*' to denote a cold state and the upper index '*warm*' to denote a warm state.

Size fractionation during deposition

Particles are transfered from the air to the snow by dry and wet deposition. Wet deposition includes all precipitation related events and is described by an effective wet deposition velocity v_w. The continuously occurring dry deposition processes include all sinks not directly related to precipitation, i.e. mainly sedimentation, impaction, and snow drift scavenging, and are summarized as an effective total dry deposition velocity v_d. We consider only multi-year means (disregarding e.g. changed seasonality of precipitation [*Werner et al.*, 2000]) and assume that the precipitation rate equals the accumulation rate; then the deposition flux is proportional to $(v_w + v_d)c_{air} = (\varepsilon A + v_d)c_{air}$ with

ε: scavenging ratio, i.e. particle concentration in new snow divided by c_{air},

A: accumulation rate, and

c_{air}: airborne particle concentration.

In a first order approximation size fractionation by dry deposition may be described as $v_d = kd^n$ (d: particle diameter, k and n: constants), although for large particles v_d may be rate limited through insufficient vertical exchange. Wet deposition may be regarded as so efficient that at least for high enough precipitation rates its size fractionating potential [*Junge*, 1977] is quenched; thus we assume ε independent from particle size. In this picture the size distribution is shifted towards larger particles by dry deposition but not by wet deposition, and consequently the resulting size distribution in the ice depends on the ratio of dry and wet deposition fluxes. Therefore, a change in the accumulation rate will change the archived size distribution (see also [*Unnerstad and Hansson*, 2001]).

The unimodal, lognormal size distribution $\langle \mu_{air}, \sigma \rangle$ with mode μ_{air} and standard deviation σ transforms during deposition as $\langle \mu_{air}, \sigma \rangle \cdot (v_w + v_d)$. The mode μ_{ice} of the size distribution in the ice is found at the maximum of this product and is given by (using the notation $\sigma_g = \ln \sigma$)

$$\ln\left(\frac{\mu_{ice}}{\mu_{air}}\right) = n\sigma_g^2 \frac{v_d}{v_w + v_d} = n\sigma_g^2 \frac{k\mu_{ice}^n}{A\varepsilon + k\mu_{ice}^n}.$$

Obviously, the maximum shift occurs if only dry deposition is active; in that extreme case $\frac{\mu_{ice}}{\mu_{air}} = \exp\left(n\sigma_g^2\right)$; and with $n = 2$ (sedimentation) and $\sigma = 1.7$ a factor of ≈ 1.7 is obtained.

Because the accumulation rate differed during different past climates the size shifts due to deposition were also different. To investigate to which extent the observed systematic changes of μ_{ice} may arise from this depositional effect we calculate the size shift for two different accumulation rates. We choose $\mu_{air} = 1.4$ μm and assume

constant values for n ($n = 2$), σ ($\sigma = 1.7$), k ($k = 8.3 \cdot 10^7$ $m^{-1}s^{-1}$ from [*Fuchs*, 1964]), and ε. The values vor ε are not well known, but $0.2{\cdot}10^6 \leq \varepsilon \leq 2.0{\cdot}10^6$ seems probable as *Davidson et al.* [1996] find $\varepsilon = (0.65 \pm 0.31) \cdot 10^6$ for Ca^{2+} at Summit. For $A^{warm} = 0.2$ ma^{-1} and $A^{cold} = 0.5A^{warm}$, which reflects LGM vs. Preboreal accumulation changes [*Johnsen et al.*, 1997], we obtain a difference $\Delta = (\mu_{ice}^{cold} - \mu_{air}^{cold}) - (\mu_{ice}^{warm} - \mu_{air}^{warm})$ of $\Delta = 0.08$ μm for $\varepsilon = 0.2 \cdot 10^6$ and $\Delta = 0.01$ μm for $\varepsilon = 2.0 \cdot 10^6$, which typically is about 1/4 of the absolute shifts $\mu_{ice} - \mu_{air}$ between airborne and deposited particles in our calculations. Similar results are achieved if more realistic calculations of v_d are used [*Sehmel*, 1980].

These calculated differences compare to our observed changes of μ_{ice} of approx. 0.4 μm for LGM vs. Holocene climatic changes. Thus, the differences in particle deposition during warm and cold climates can only account for roughly 3% to 20% of the observed change of μ. We therefore conclude that the observed differences of μ during different climatic periods predominantly reflect changed airborne size distributions over Greenland. (See Figure 7 for an illustrative sketch.)

Size fractionation during emission, uplift and long range transport

Emission According to *Gillette et al.* [1974] the wind speed has little influence on the size distribution in the range from 2-10 μm. And also *D'Almeida and Schütz* [1983] find that dust storms do not change the size distribution of airborne mineral dust particles below 10 μm diameter. Only above 10 μm the abundance of large particles increases during high surface winds. Because we consider only particles smaller than 10 μm we assume the size distribution of airborne particles a few meters above the ground as independent from the source strength. The mode of this distribution be μ_{source}.

Uplift and long range transport The change of particle concentration during transport can be described by the term $f \cdot e^{-t/\tau}$, with
t: transit time between free troposphere at source and deposition onto the ice sheet,
τ: residence time governed by depletion processes en route, and
f: correction factor in our one-dimensional approach to account for external mixing with particle free air (dilution).
Size fractionating depletion processes may be accounted for by allowing the residence time to be size dependent, i.e. $\tau = \tau(d)$. For long range transport we assume $\tau(d) = \frac{H}{\tilde{v}_w + \tilde{v}_d}$, where H denotes the mixing height, $\tilde{v}_w$ describes the depletion process due to wet depletion en route and $\tilde{v}_d$ due to dry depletion en route. Note that for the depletion

processes during transport considered here $\tilde{v}_w$ and $\tilde{v}_d$ may be very different from the deposition velocities v_w and v_d at the ice sheet considered earlier. Dry deposition again is assumed to be size fractionating according to $\tilde{v}_d = kd^n$, and also here $\tilde{v}_w$ is assumed to be so efficient that its size fractionating character is overridden. Any size fractionating portions of $\tilde{v}_w$ that possibly remain may be treated as increased dry depletion in this picture.

Following the motion of an air parcel, an unimodal, lognormal size distribution $\langle \mu_0, \sigma \rangle$ transforms as $\langle \mu_0, \sigma \rangle \cdot f \cdot e^{-t\frac{\tilde{v}_w + \tilde{v}_d}{H}}$. The resulting distribution is not necessarily exactly lognormal; however, the new mode μ, which again is found at the maximum of this product, is characterized by:

$$\ln\left(\frac{\mu}{\mu_0}\right) = -n \cdot \sigma_g^2 \cdot \frac{t}{\tau} \frac{\tilde{v}_d}{\tilde{v}_w + \tilde{v}_d} \tag{1}$$

which means that μ decreases with time. Simultaneously the distribution gets narrower, i.e. σ_g also decreases. Consequently, the change of μ is more rapid at the beginning when σ_g is large.

We now compare the size change during long range transport at a cold and warm climatic state. To meet problems from possibly different uplift rates during cold and warm climates we define long range transport to start once a reference size distribution with the mode μ_{ref} is reached in the free troposphere. Thus, by definition, in our model picture $\mu_{ref}^{cold} = \mu_{ref}^{warm}$. This may also be the case in reality, however, our current knowledge about this is poor. If the uplift rates were different during cold and warm climatic states then in one state the air parcel will already have travelled farther until μ_{ref} is reached, thus reducing somewhat the distance to be covered by long range transport. However, since the horizontal displacement during uplift is small compared to the distance to be covered by long range transport and since the mode changes relatively quickly at the beginning a possible difference in uplift will have only a small adverse effect on our model results.

In this picture the ratio $\frac{\mu_{air}^{cold}}{\mu_{air}^{warm}}$ of the airborne modes at the ice sheet can be deduced from equation 1 as

$$\ln\left(\frac{\mu_{air}^{cold}}{\mu_{air}^{warm}}\right) = -\ln\left(\frac{\mu_{air}^{warm}}{\mu_{ref}^{warm}}\right)\left[1 - \frac{c_1 c_2 c_3}{c_4}\frac{t^{cold}}{t^{warm}}\right] \tag{2}$$

where $c_1 = (\sigma_g^{cold}/\sigma_g^{warm})^2$, $c_2 = n^{cold}/n^{warm}$, $c_3 = \tilde{v}_d^{cold}/\tilde{v}_d^{warm}$, and $c_4 = H^{cold}/H^{warm}$. With the assumption of identical initial widths of distributions ($c_1 = 1$), dry deposition mechanisms ($c_2 = 1$), dry deposition strengths ($c_3 = 1$), and mixing heights ($c_4 = 1$) equation 2 directly links $\mu_{air}^{cold}/\mu_{air}^{warm}$ with t^{cold}/t^{warm}. Figure 6 shows the thus derived

ratios of t^{cold}/t^{warm} as a function of μ^{cold}/μ^{warm} due to changes in transport. Since we have only limited knowledge about μ_{ref}, three different values have been applied for $\mu_{air}^{warm}/\mu_{ref}^{warm}$: All are based on $\mu_{air}^{warm} = 1.3$ μm, which is on average our measured mode during Preboreal; μ_{ref}^{warm} has been taken as 2.5 μm, 3.2 μm and 4.0 μm respectively. 2.5 μm surely imposes a lower limit on μ_{ref}^{warm} as this value is found in high Alpine ice cores during Saharan dust events [*Wagenbach and Geis*, 1989]; on the other hand 4.0 μm diameter may be deduced as an upper limit from [*D'Almeida and Schütz*, 1983]. The intermediate value of 3.2 μm may therefore give a good estimate for μ_{ref}. In Figure 6 typical ratios of $\mu_{air}^{cold}/\mu_{air}^{warm}$ have been marked for LGM vs. Preboreal and Stadial vs. Interstadial climate changes whereby it is assumed that differences in long range transport account for our observed changes of μ after a 10 % correction for different deposition scenarios was made. With these assumptions the implied ratio of transit times can be read from Figure 6. A ratio $t^{cold}/t^{warm} \approx 0.75$ is suggested from our model picture for the LGM vs. Preboreal and $t^{cold}/t^{warm} \approx 0.9$ for the Stadial vs. Interstadial comparison. The difference between a cold and a warm state is illustratively sketched in Figure 7.

Implications from size changes for concentration changes

The evidence we found for the ratio of transit times t^{cold}/t^{warm} imposes limits on the concentration change associated with changed long range transport. The concentration change resulting from different long range transport during cold and warm periods may be written as $\left(\frac{C^{cold}}{C^{warm}}\right) = \frac{f^{cold}}{f^{warm}} \cdot \exp\left(\frac{t^{warm}}{\tau^{warm}}\left(1 - \frac{\tau^{warm}}{\tau^{cold}}\frac{t^{cold}}{t^{warm}}\right)\right)$. To calculate C^{cold}/C^{warm} as a function of t^{cold}/t^{warm} a number of estimates are necessary. For the dilution with particle free air $f \sim 1/s$ is taken where s is the transversal width of the transported dust plume. Supposing $s = \sqrt{D/t}$ and no change of eddy diffusion constants D renders $f^{cold}/f^{warm} = (t^{cold}/t^{warm})^{-1/2}$. The scaling factor t^{warm}/τ^{warm} can be estimated from equation 1 by taking $\frac{\mu}{\mu_0} = \frac{\mu_{air}^{warm}}{\mu_{ref}^{warm}} \approx \frac{1.3\mu m}{3.2\mu m}$, $n = 2$, $\sigma_g = \ln 1.7$, and by assuming $\tilde{v}_d \approx \tilde{v}_w$ during warm climates (i.e. in our picture: equal portions of size fractionating and non-fractionating loss processes); this renders $\frac{t^{warm}}{\tau^{warm}} = 3.2$. Further, the ratio of residence times τ^{warm}/τ^{cold} may be estimated by supposing equal mixing heights $H^{cold} = H^{warm}$ and dry depletion velocities $\tilde{v}_d^{cold} = \tilde{v}_d^{warm}$ and by assuming $\tilde{v}_w^{cold} = 0.5\tilde{v}_w^{warm}$ for LGM vs. Preboreal to account for reduced wet depletion en route during LGM; the latter appears a reasonable upper estimate from extrapolating the observed reduction of the accumulation rate to the entire transport path as well as from model calculations of the hydrological cycle [*Andersen and Ditlevsen*, 1998]; this yields $\tau^{warm}/\tau^{cold} = 0.75$.

In Figure 8 the resulting C^{cold}/C^{warm} is shown as a function of t^{cold}/t^{warm} for

two scenarios of τ^{warm}/τ^{cold}: First, $\tau^{warm}/\tau^{cold} = 1$ is taken for curve (A), which shows C^{cold}/C^{warm} resulting from changed transit times only. For curve (B) also the residence times were varied, which is more realistic; $\tau^{warm}/\tau^{cold} = 1$ is presumed for no change of circulation ($t^{cold}/t^{warm} = 1$) and $\tau^{warm}/\tau^{cold} = 0.75$ for LGM vs. Preboreal changes ($t^{cold}/t^{warm} = 0.75$) with a linear interpolation in between. This gives values for C^{cold}/C^{warm} of ≈ 5 for LGM vs. Preboreal and ≈ 2 for a typical D/O transition.

Summary of model results

Our simple 1-D model picture considers size fractionation during particle deposition and long range transport. We conclude that due to size fractionation during dry deposition the size distribution is shifted towards larger particles in the ice with respect to the air. This shift was larger during cold climates when wet deposition was lower. However, the difference in shift between cold and warm climates may account only for around 3% to 20% of the particle size changes we observe in the ice. Therefore, changes of μ during different climatic periods predominantly reflect changed airborne size distributions over Greenland.

We find that the size distribution may be influenced strongly by size fractionating depletion processes during long range transport, which lead to a shift towards smaller particles at the deposition site compared to the source. Therefore, shorter transit times during colder climates would lead to larger airborne particles at the ice sheet and could explain the observed mode changes between cold and warm climates. Our model picture only allows for a rough quantitative evaluation of this effect: Demanding that the observed mode change (after a 10% correction due to the deposition effect was made) is solely due to changed long range transport during cold and warm climates implies a change of transit times of $t^{cold}/t^{warm} \approx 0.75$ for LGM vs. Preboreal and $t^{cold}/t^{warm} \approx 0.9$ for D/O changes.

These changes of transit times are associated with changes of airborne concentration at the ice sheet relative to the source. These again can be estimated roughly, which yields a factor ≈ 5 concentration increase for LGM vs. Preboreal and a factor ≈ 2 for Stadial vs. Interstadial. Given the observed concentration increase in our data by a factor of 100 from Preboreal to LGM it is evident even from our rough estimate that other processes must have contributed more effectively to the concentration increase than did changes of atmospheric circulation. These other processes may have included source strength intensification through an increased frequency of dust storms, higher surface wind speeds or increased source aridity, as these do not cause a change of the size distribution in our model picture.

From ice cores and from other paleoclimatic archives it has been inferred that atmospheric circulation during the last glacial period substantially differed from present day's, e.g. [*Janecek and Rea*, 1985; *Rea*, 1994; *Kapsner et al.*, 1995; *Lamy et al.*, 1999; *Lagroix and Banerjee*, 2002]; in particular, increased westerly flow has been proposed for both the northern and the southern hemispheres. Higher wind speeds during the LGM are also proposed from modelling exercises. *Andersen and Ditlevsen* [1998] as well as *Tegen and Rind* [2000] calculated the increase of airborne dust concentration due to higher wind speed and a reduced hydrological cycle during the LGM compared to present day and suggest factors of around 2 to 4. The similarity of these values to our estimates supports the hypothesis that a change in transit times not only bares the potential of changing the particle size distribution in polar ice cores but in fact was the controlling mechanism.

Comparison with other ice core records

Much attention has been given to the question "whether particles were larger during Holocene or LGM". However, this unspecific formulation allows for several confusions. Firstly, the answer depends on the size parameter that is considered because various size parameters behaved differently. In our data set we find instances where, for example, the lognormal mode increases, absolute coarseness stays unchanged, relative coarseness decreases, and the mean volume diameter remains unchanged. Therefore, the size parameter which is considered must always be specified. Secondly, the stated question may be confused with the one "whether particles were larger in conjunction with high or with low particle concentrations"; the necessity for this differentiation has become apparent at least for Antarctica from recent work (see below).

Regarding the dependance of the lognormal mode on the particle concentration, the observations in the Greenlandic Dye3 [*Steffensen*, 1995] and GRIP [*Steffensen*, 1997] ice cores during the last glacial resemble each other closely with respect to both rate of increase as well as absolute level (see Figure 9). In the NGRIP core we find a similar rate of increase, but a lower absolute level, which may be due to methodical or unknown geographical differences. For Antarctica, in early size distribution measurements, *Petit et al.* [1981] and *De Angelis et al.* [1984] did not perform lognormal fits, but an optical inspection of their data suggested increasing modes with increasing concentration, which is sketched in Figure 9. Both find this trend for glacial as well as for Holocene samples. However, new Antarctic data by *Delmonte et al.* [2002] contains increasing modes with increasing concentration only for glacial ice older than the Antarctic Cold

Reversal. Yet unexplained, the opposite behavior is clearly exhibited for younger ice, which may be an important clue for the understanding of past southern hemisphere climate. This opposite behavior leads to the phenomenon that although particle modes increase with concentration in pleistocene ice still they are larger during Holocene than during LGM. This probably had not been observed in the earlier Antarctic work [*Petit et al.*, 1981; *De Angelis et al.*, 1984] due to limited number and non-representative selection of samples. For Greenland there is not enough Holocene data to confirm or exclude such a subdivided behavior. The larger absolute values of μ in Antarctica compared to Greenland may result from higher contribution of dry deposition due to a lower accumulation rate at the Antarctic sites.

Regarding the relative coarseness, a greater relative abundance of large particles concurrent with high concentrations had been reported for Antarctica [*Petit et al.*, 1981] but a smaller one for Greenland [*Steffensen*, 1997]. However, like *Steffensen* [1997] also *Delmonte et al.* [2002] find less large particles during times of high concentrations. Since this new data due to methodical differences has a higher resolution than that of *Petit et al.* [1981], the disagreement seems to be resolved. Also we find relatively less large particles at high concentrations, so that it seems evident that relative coarseness changed similarly in Greenland and Antarctica. Although findings for Greenland and Antarctica are in accordance at least during the glacial epoch the atmospheric systems transporting dust to the polar ice sheets may have behaved very differently in the northern and southern hemispheres; whereas in Antarctica the abundance of large particles clearly must be driven by atmospheric transport, in Greenland also other causes such as varying contributions of proximal sources or of biological particles may be important.

Conclusions

This study shows that a laser particle detector can be used for very efficient counting and sizing of windblown mineral microparticles in ice cores. A more than 1500 m long continuous profile is provided covering in 1.65 m resolution almost the complete last glacial period. We find particle concentrations higher by a factor of 100 during LGM than during the Preboreal and concentration changes by typically a factor of 8 at the sharp transitions of D/O-events. The mode μ of the lognormal size distribution varies systematically with the tendency towards smaller particles during warmer climates. The variability of the mode is higher during warmer climates, and values of the standard deviation σ are also increased; the latter results from increased variability of the size

distributions of the events that contribute particles to each multi-year sample.

We base our interpretation of the particle size distribution on a highly simplified, but quantitative model picture. From this we interpret the lognormal mode as indicating atmospheric transit times during long range transport from the source to the ice sheet. Larger modes indicate shorter transit times, which may result from higher mean advection velocities and/or shorter transport routes. Both may be related to the position of the Polar Front. From our data we conclude roughly 25% shorter transit times during LGM than during the Preboreal. As we find that circulation changes alone clearly cannot account for the observed concentration increase by a factor of 100 other processes such as source intensification must have contributed synchronously. This means that climatic situations lead to increased source strength as well as to shorter transit times during cold periods. The clear correlation of processes in the source areas with large scale atmospheric circulation patterns suggests strong mediating mechanisms.

During warm periods a clear tendency towards longer transit times is exhibited. However, transit times were much more variable and occasionally also have been short. It therefore appears that atmospheric regimes providing slower transport were more variable and on the contrary that atmospheric circulation was more confined during cold climates. This may reveal the variability of the Polar Front with respect to the source areas: During cold periods the Polar Front may have always been located far enough south to include the source areas. Whereas during warmer periods the Polar Front may have been located generally further north but was subject to occasional southward excursions.

The variability of transit times during warm periods is – on time scales of up to several 100 years – not connected to variable source strength. This certain degree of independence between dust production processes and long range transport times is observed despite their generally strong linkage. The independence is also evident from occasional timing differences of dust concentration and size distribution parameters at rapid climatic transitions. This underlines that source processes by themselves do not influence the size distribution of particles carried to Greenland. It further suggests that both source processes and long range transport are two independent results from environmental forcings.

Clearly, the interpretation of particle size distributions in ice cores is still limited through our insufficient understanding of size fractionating processes. Sophisticated model calculations for long range transport and particle deposition are needed to check our findings and to draw more differentiated conclusions from the size distribution data. Size distribution measurements at high depth resolution may aid the understanding of rapid climate transitions during the last glacial period. Furthermore, an investigation

of size distributions in Greenland during the Holocene are desirable for a comparison to the newest Antarctic results. As insights on variability, timing and the systematics of changes are benefits from continuous measurements, these should always be preferred over spot-check type investigations.

Acknowledgements
The North-GRIP project is directed and organized by the Department of Geophysics at the Niels Bohr Institute for Astronomy, Physics and Geophysics, University of Copenhagen. It is being supported by funding agencies in Denmark(SNF), Belgium (NFSR), France (IFRTP and INSU/CNRS), Germany (AWI), Iceland (RannIs), Japan (MECS), Sweden (SPRS), Switzerland (SNF) and the United States of America (NSF). We wish to thank all the funding bodies and field participants. Matthias Bigler and Regine Röthlisberger are acknowledged for their exceptional dedication in running the CFA-lab in the field. Hubertus Fischer is thanked for his helpful comments to the manuscript.

References

Andersen, K. K., A. Armengaud, and C. Genthon, Atmospheric dust under glacial and interglacial conditions, *Geophysical Research Letters, 25*(13), 2281–2284, 1998.

Andersen, K. K., and P. D. Ditlevsen, Glacial - interglacial variations of meridional transport and washout of dust: A one-dimensional model, *Journal of Geophysical Research, 103*(D8), 8955–8962, 1998.

Biscaye, P. E., F. E. Grousset, M. Revel, S. Van der Gaast, G. A. Zielinski, A. Vaars, and G. Kukla, Asian provencance of glacial dust (stage 2) in the greenland ice sheet project 2 ice core, summit, greenland, *Journal of Geophysical Research, 102*(C12), 26765–26781, 1997.

Chylek, P., G. Lesins, and U. Lohmann, Enhancement of dust source area during past glacial periods due to changes of the hadley circulation, *Journal of Geophysical Research, 106*(D16), 18,477–18,485, 2001.

Cragin, J. H., M. M. Herron, C. C. J. Langway, and G. Klouda, Interhemisheric comparison of changes in the composition of atmospheric precipitation during the late cenozoic era, in *Polar Oceans*, edited by M. J. Dunbar, pp. pp.617–631, Arct. Inst. of North America, Calgary, AB, Canada, 1977.

D'Almeida, Guillaume, A., and L. Schütz, Number, mass and volume distributions of mineral aerosol and soils of the sahara, *Journal of Climate and Applied Meteorology, 22*, 233–243, 1983.

Davidson, C. I., M. H. Bergin, and H. D. Kuhns, The deposition of particles and gases to ice sheets, in *Chemical Exchange Between the Atmosphere and Polar Snow*, edited by E. W. Wolff and R. C. Beales, pp. 275–306, Springer Verlag, Berlin Heidelberg, 1996.

De Angelis, M., M. Legrand, J. R. Petit, N. I. Barkov, Y. S. Korotkevitch, and V. M. Kotlyakov, Soluble and insoluble impurities along the 950 m deep vostok ice core (antarctica) - climatic implications, *Journal of Atmospheric Chemistry, 1*, 215–239, 1984.

Delmonte, B., J. R. Petit, and V. Maggi, Glacial to Holocene implications of the new 27,000-year dust record from the EPICA Dome C (East Antarctica) ice core., *Climate Dynamics,*, in press, 2002.

Fuchs, N. A., *The machanics of aerosols*, Pergamon Press, Oxford, London, Edinburgh, New York, Paris, Frankfurt, 1964.

Fuhrer, K., E. W. Wolff, and S. J. Johnsen, Timescales for dust variability in the Greenland Ice Core Projct (GRIP) ice core in the last 100,000 years, *Journal of Geophysical Research, 104*(D24), 31043–31052, 1999.

Gillette, D. A., J. Adams, A. Endo, and D. Smith, Threshold velocities for input of soil particles into the air by desert soils, *Journal of Geophysical Research, 85*(C10), 5621–5630, 1980.

Gillette, D. A., I. H. J. Blifford, and D. W. Fryrear, The influence of wind velocity on the size distributions of aerosols generated by the wind erosion of soils, *Journal of Geophysical Research, 79*(27), 4068–4075, 1974.

Grootes, P. M., and M. Stuiver, Oxygen 18/16 variability in Greenland snow and ice with 10-3 - to 10-5 -year time resolution, *Journal of Geophysical Research, 102*(C12), 26,455–26,470, 1997.

Hammer, C. U., H. B. Clausen, W. Dansgaard, A. Neftel, P. Kristinsdottir, and E. Johnson, Continuous impurity analysis along the dye 3 deep core, in *Greenland Ice Core: Geophysics, Geochemistry, and the Environment*, edited by C. C. J. Langway, H. Oeschger, and W. Dansgaard (Eds.), Volume 33 of *Geophysical Monograph 33*, pp. 90–94, American Geophysical Union, Washington, 1985.

Hansson, M. E., The Renland ice core. A Nothern hemisphere record of aerosol composition over 120'000 years, *Tellus, 46B*, 390–418, 1994.

Janecek, T. R., and D. K. Rea, Quaternary fluctuations in the northern hemisphere trade winds and westerlies, *Quaternary Reasearch, 24*, 150–163, 1985.

Johnsen, S. J., H. B. Clausen, W. Dansgaard, N. S. Gundestrup, C. U. Hammer, U. Andersen, K. K. Andersen, C. S. Hvidberg, D. Dahl-Jensen, J. P. Steffensen, H. Shoji, A. E. Sveinbjrnsdttir, J. W. C. White, J. Jouzel, and D. Fisher, The δ^{18}O record along the Greenland Ice Core Project deep ice core and the problem of possible eemian climatic instability, *Journal of Geophysical Research, 102*(C12), 26397–26410, 1997.

Junge, C. E., Processes responsible for the trace content in precipitation, in *Isotopes and Impurities in Ice and Snow*, IAHS-AISH publication no. 118, Grenoble, 1977.

Kahl, J. D. W., D. A. Martinez, H. Kuhns, C. I. Davidson, J.-L. Jaffrezo, and J. M. Harris, Air mass trajectories to summit, greenland: A 44-year climatology and some episodic events, *Journal of Geophysical Research, 102*(C12), 26,861–26,875, 1997.

Kapsner, W. R., R. B. Alley, C. A. Shuman, S. Anandakrishnan, and P. M. Grootes, Dominant influence of atmospheric circulation on snow accumulation in greenland over the past 18,000 years, *Nature, 373*, 52–54, 1995.

Krinner, G., and C. Genthon, GCM simulations of the Last Glacial Maximum surface climate of Greenland and Antarctica, *Climate Dynamics, 14*, 741–758, 1998.

Lagroix, F., and S. K. Banerjee, Paleowind directions from the magnetic fabric of loess profiles in central alaska, *Earth and Planetary Science Letters, 195*, 99–112, 2002.

Lamy, F., D. Hebbeln, and G. Wefer, High-resolution marine records of climatic change in mid-latitude chile during the last 28,000 years based on terrigenous sediment parameters, *Quaternary Research, 51*, 83–93, 1999.

Mahowald, N., K. Kohfeld, M. Hansson, Y. Balkanski, S. P. Harrison, I. C. Prentice, M. Schulz, and H. Rodhe, Dust sources and deposition during the last glacial maximum and current climate: A comparison of model results with paleodata from ice cores and marine sediments, *Journal of Geophysical Research, 104*(D13), 15895–15916, 1999.

Petit, J.-R., M. Briat, and A. Royer, Ice age aerosol content from east antarctic ice core samples and past wind strenght, *Nature, 293*, 391–394, 1981.

Petit, J. R., L. Mounier, J. Jouzel, Y. S. Korotkevich, V. I. Kotlyakov, and C. Lorius, Palaeoclimatological and chronological implications of the vostok core dust record, *Nature, 343*, 56–58, 1990.

Porter, S. C., and A. Zhisheng, Correlation between climate events in the north atlantic and china during the last glaciation, *Nature, 375*, 305–308, 1995.

Pye, K., *Aeolian dust and dust deposits*, Academic Press, London, 1987.

Rea, D. K., The paleoclimatic record provided by eolian deposition in the deep sea: The geologic history of wind, *Reviews of Geophysics, 32*(2), 159–195, 1994.

Röthlisberger, R., M. Bigler, A. Hutterli, S. Sommer, B. Stauffer, H. G. Junghans, and D. Wagenbach, Technique for continious high-resolution analysis of trace substances in firn and ice cores, *Environmental Science Technology, 34*, 338–342, 2000.

Royer, A., M. De Angelis, and J. R. Petit, A 30000 year record of physical and optical properties of microparticles from an east antarctic ice core and implications for paleoclimate reconstruction models, *Climate Change, 4*, 381–412, 1983.

Ruth, U., D. Wagenbach, M. Bigler, J. P. Steffensen, and R. Röthlisberger, High resolution dust profiles at NGRIP: Case studies of the calcium-dust relationship, *Annals of Glaciology, 35*, in press, 2002.

Saey, P., 1998, *Concentration and size distribution of microparticles in Alpine and polar ice cores (in German)*, M.sc. thesis, University of Heidelberg.

Sehmel, G. A., Particle and gas dry deposition: A review, *Atmospheric Enviroment, 14*, 983–1011, 1980.

Steffensen, J. P., 1995, *Microparticles and chemical impurities in ice cores from Dye 3, South Greenland and their interpretation in palaeoclimatic reconstructions*, Ph.d. thesis, University of Copenhagen.

Steffensen, J. P., The size distribution of microparticles from selected segments of the greenland ice core project ice core representing different climatic periods, *Journal of Geophysical Research, 102*(C12), 26,755–26,763, 1997.

Sugimae, A., Elemental constituents of atmospheric particulates and particle density, *Nature, 307*, 145–147, 1984.

Svensson, A., P. E. Biscaye, and F. E. Grousset, Characterization of late glacial continental dust in the greenland ice core projct ice core, *Journal of Geophysical Research, 105*(D24), 4637–4656, 2000.

Tegen, I., and I. Fung, Modeling of mineral dust in the atmosphere: Sources, transport, and optical thickness, *Journal of Geophysical Research, 99*(D11), 22897–22914, 1994.

Tegen, I., and D. Rind, Influence of the latitudinal temperature gradient on soil dust concentration and deposition in greenland, *Journal of Geophysical Research, 105*(D6), 7199–7212, 2000.

Unnerstad, L., and M. Hansson, Simulated airborne particle size distributions over greenland during last glacial maximum, *Geophysical Research Letters, 28*(2), 287–290, 2001.

Wagenbach, D., and K. Geis, The mineral dust record in a high altitude Alpine glacier (Colle Gnifetti, Swiss Alps), in *Paleoclimatology and Paleometeorology: Modern and Past Patterns of Global Atmospheric Transprot*, edited by M. Leinen and Sarnthein, pp. 543–564, Kluwer, 1989.

Wang, Y. J., H. Cheng, R. L. Edwards, Z. S. An, J. Y. Wu, C.-C. Shen, and J. A. DOrale, A high-resolution absolute-dated late pleistocene monsoon record from hulu cave, china, *Science, 294*(2345-2348), 2345–2348, 2001.

Werner, M., U. Mikolajewicz, M. Heimann, and G. Hoffmann, Borehole versus isotope temperatures on greenland: Seasonality does matter, *Geophysical Research Letters, 27*(5), 723–726, 2000.

Wurzler, S., T. G. Reisin, and Z. Levin, Modification of mineral dust particles by cloud processing and subsequent effects on drop size distributions, *Journal of Geophysical Research, 105*(D4), 4501–4512, 2000.

Zielinski, G. A., Paleoenvironmental implications of the insolubable microparticle record in the GISP2 (Greenland) ice core during the rapidly changing climate of the Pleistocene-Holocene transition, *Geological Society of America Bulletin, 109*(5), 547–559, 1997.

Figures

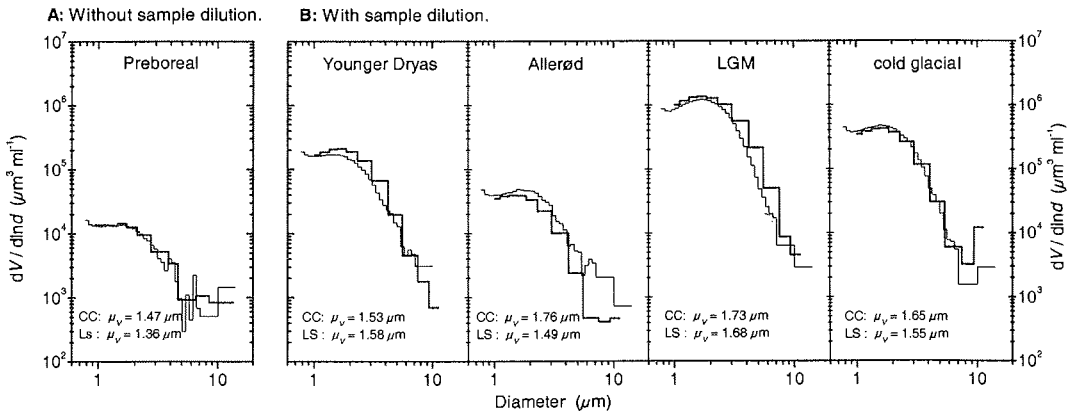

Figure 1: Size distributions by volume used for calibration. Coulter Counter (CC) data in thin lines, laser sensor (LS) data in bold lines. The laser sensor data is shown after the adjustment of its size axis. The rise at the left end of the Coulter Counter curves is due to baseline noise as the lower size limit is reached. Listed is also the lognormal mode μ of the distributions as derived from CC and LS data. Measurements without sample dilution were calibrated using the Preboreal horizon (A); measurements with sample dilution were calibrated using the other four horizons (B).

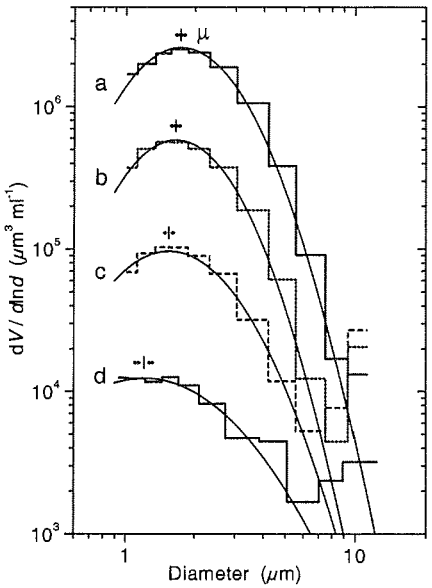

Figure 2: Individual size distributions by volume from different climatic periods along with lognormal fits. a: 1831.50 - 1833.15 m (LGM); b: 2075.70 - 2077.35 m (S9); c: 2121.90 - 2123.55 m (IS10); d: 1460.25 - 1461.90 m(Preboreal). Indicated is the position of the mode μ and the uncertainty of the fit.

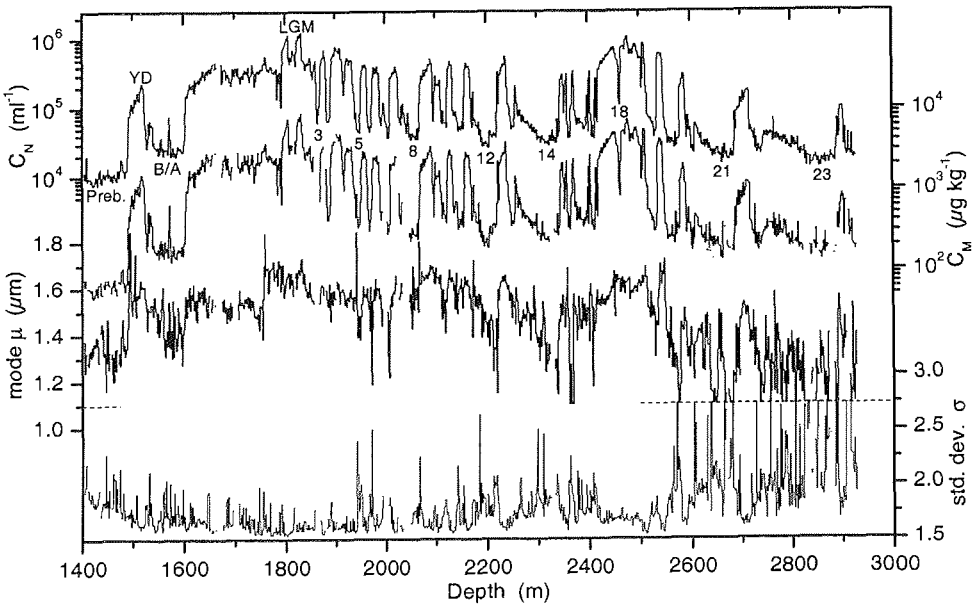

Figure 3: Profiles of microparticle concentration and lognormal size distribution parameters μ (diameter) and σ. Number concentration is based on counts of particles larger 1.0 μm. Gaps arise either from missing data or from data that did not allow for a proper lognormal fit. Selected climatic periods are labeled: Preb = Preboreal Holocene, YD = Younger Dryas, B/A = Bølling/Allerød, LGM = Last Glacial Maximum; numbers refer to Dansgaard/Oeschger-events. The data of the bottom two panels was truncated at the dashed line indicated.

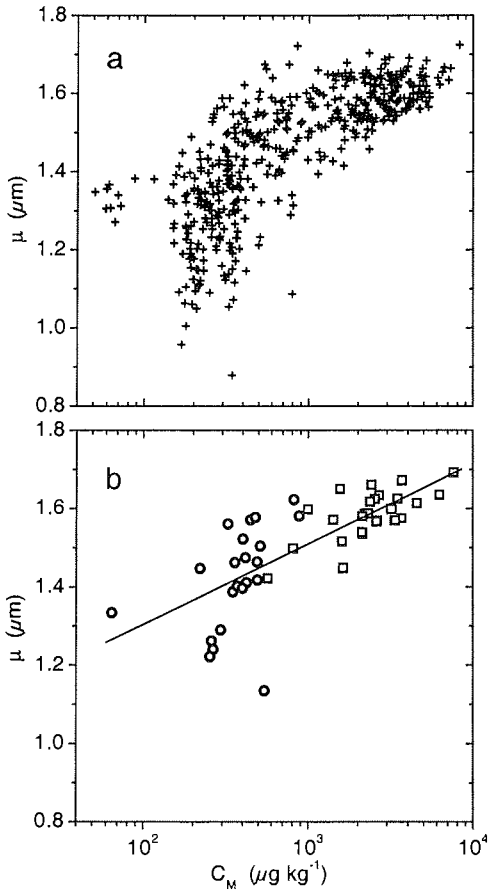

Figure 4: Correlation of the mode μ and the mass concentration C_M. a: All data has been averaged such that each data point represents 200 years. b: All data has been averaged over climatic periods; circles denote warm periods, squares denote cold periods. A logarithmic trend line is also shown.

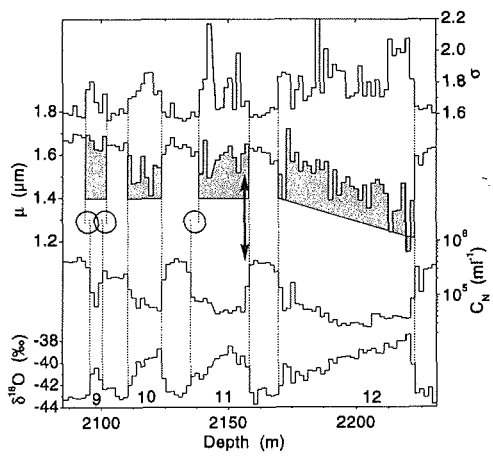

Figure 5: Detail from profiles showing various rapid D/O-transitions. Shown are size distribution parameters σ and μ number concentration C_N, and δ^{18}O (data is personal communication from NGRIP-members). Shaded areas emphasize interstadials in the profile of the mode. Circles mark instances where the timing of a transition may be inferred differently from μ and σ or respectively from V_N and δ^{18}O. The arrow points to a transition where μ seemingly shows other timing than σ. Numbers in the bottom panel indicate interstadials.

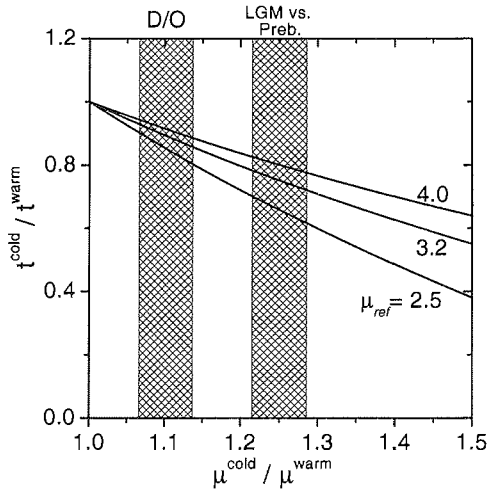

Figure 6: Implications for the change in transit times t^{cold}/t^{warm} from observed size changes μ^{cold}/μ^{warm}. Curves consider different scenarios for μ_{ref}. Shaded areas mark LGM vs. Preboreal and Stadial vs. Interstadial (D/O) changes, respectively.

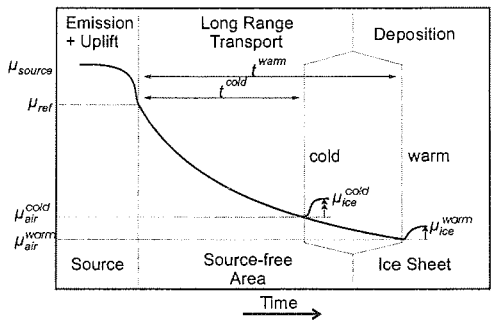

Figure 7: Schematic illustration to the model picture. The airborne particle size distribution with mode μ_{source} at the source is changed rapidly during uplift until μ_{ref} is reached. Here, per definition, long range transport across source-free areas starts. During long range transport the mode decreases slowly owing to size fractionating depletion processes. Because the transit time t during cold climates is shorter than during warm climates the mode μ_{air} of airborne particles at the ice sheet is larger during cold climates. During deposition the mode is shifted slightly towards larger particles leading to μ_{ice}. Upper indices '*cold*' and '*warm*' denote cold and warm climatic states, respectively.

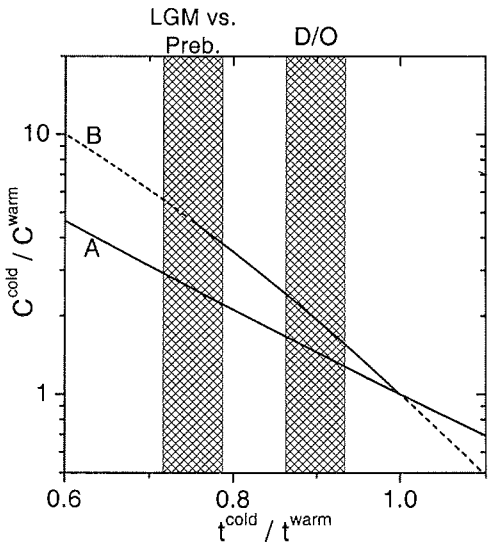

Figure 8: C^{cold}/C^{warm} as a function of t^{cold}/t^{warm} for two scenarios of τ^{warm}/τ^{warm}. (A): no change of residence times; (B): reduction of wet removal during LGM as described in the text; extrapolations are dashed. Shaded areas mark probable values for t^{cold}/t^{warm} for LGM vs. Preboreal and D/O transitions as inferred from Figure 6.

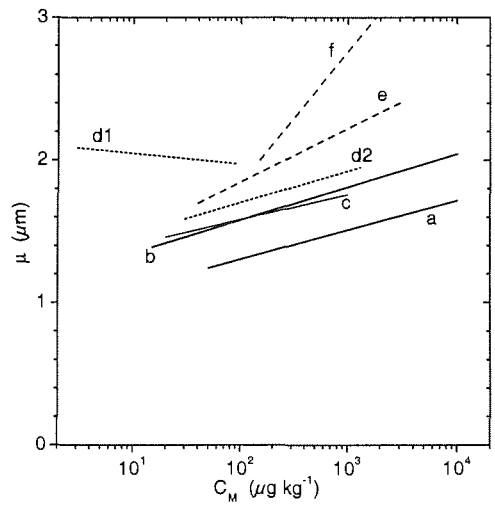

Figure 9: Correlation of C_M and μ in different ice cores from Greenland (solid lines) and from Antarctica (broken lines). a: NGRIP, this work; b: GRIP [*Steffensen*, 1997]; c: Dye3 [*Steffensen*, 1995]; d1: EPICA Dome-C, Holocene data until mid-transition including Antarctic Cold Reversal (ACR) [*Delmonte et al.*, 2002]; d2: EPICA Dome-C, glacial data starting mid-transition excluding ACR) [*Delmonte et al.*, 2002]; e: Dome-C (Holocene and glacial samples) [*Petit et al.*, 1981]; f: Vostock (Holocene and glacial samples) [*De Angelis et al.*, 1984]. For (e) and (f) mass concentrations were inferred from the number concentrations reported using a conversion deduced from [*Delmonte et al.*, 2002].